J Neuropathol Exp Neurol
Vol. 68, No. 12
December 2009
pp. 1269–1281

ORIGINAL ARTICLE

Effects of 4-Methylcatechol on Skin Reinnervation: Promotion of Cutaneous Nerve Regeneration After Crush Injury

Yu-Lin Hsieh, PhD, Whei-Min Lin, MS, June-Horng Lue, PhD, Ming-Fong Chang, MS, and Sung-Tsang Hsieh, MD, PhD

Abstract

We assessed the effects of treatment with 4-methylcatechol (4MC), a known inducer of nerve growth factor, on peripheral nerve regeneration by analyzing cutaneous and muscular reinnervation in mice after sciatic nerve crush injury. At 3 months postinjury, the skin innervation index was significantly higher in the 4MC group than the control group ($p = 0.0002$); there was also increased unmyelinated fiber density ($p = 0.0042$) and unmyelinated fibers/Remak bundle ($p = 0.001$) in sural nerves, indicating unmyelinated nerve fiber regeneration. These changes were accompanied by increases of transcripts for nerve growth factor ($p = 0.0026$) and glial cell line–derived neurotrophic factor ($p = 0.03$) in the 4MC group. In contrast, muscle innervation indices were similar in both groups and were higher than the skin innervation index ($p < 0.0001$). The regeneration of myelinated nerve fibers, as assessed by fiber density, diameter and *g* ratio analyses in sural nerves, and amplitudes of muscle action potential in sciatic nerves, was similar in both groups. Taken together, these data suggest that 4MC specifically promoted the regeneration of unmyelinated nerve fibers and reinnervation of the skin by increasing the expression of nerve growth factor and glial cell line–derived neurotrophic factor.

Key Words: 4-Methylcatechol, Glial cell line–derived neurotrophic factor, Muscle reinnervation, Nerve growth factor, Neurotrophins, Regeneration, Skin reinnervation.

INTRODUCTION

Despite significant progress in understanding peripheral nerve regeneration, whether the degrees of cutaneous and muscular reinnervation are the same after nerve injury and whether the nerve growth factor (NGF) inducer 4-methylcatechol (4MC) can promote regeneration of small-diameter sensory nerves terminating in the skin are not known. Although regeneration of nerve fibers occurs across transection sites after injury, correctly targeted reinnervation by directional outgrowth continues to be insufficient for good functional recovery after peripheral nerve injury (1, 2). For example, the administration of lentivirus-mediated NGF and glial cell line–derived neurotrophic factor (GDNF) alters the expression patterns of dorsal root ganglion neurons and presumably improves motor regeneration, as assessed by gastrocnemius muscle weight (3); however, direct evidence that the muscles truly became reinnervated is lacking. Thus, it is important to evaluate the reinnervation target after peripheral nerve injury to assess successful nerve regeneration (1, 2). Only limited studies have explored the morphological evidence of targeted reinnervation such as of muscle through nerve conduits after sciatic nerve transection (4).

Peripheral nerves are composed of motor and sensory fibers. Most studies assessing the morphometry of the sciatic nerve raise 2 questions: "Do the target tissues become reinnervated?" and "Do motor and sensory nerves regenerate to a similar degree?" The sensory innervation of the skin can be assessed by demonstrating intraepidermal nerve fibers using various axonal markers (5, 6). Therefore, the integration of these approaches for analysis of muscular and cutaneous innervation will permit comparison of regeneration of motor and sensory nerves after nerve injury.

Regeneration of peripheral nerves subsequent to degeneration after injury occurs in experimental animals (1, 7). Nerve regeneration, however, is a challenge in humans because various underlying conditions such as diabetes can hinder the regeneration of peripheral nerves after injury (8–11). Sensory nerve degeneration is a major clinical problem, and there is no satisfactory therapy for it despite some applications of gene therapy such as of vascular endothelial growth factor (11, 12). The use of a simple small molecule for sensory nerve regeneration treatment is the goal. We previously demonstrated that 4MC enhances sensory nerve regeneration and cutaneous reinnervation in a mouse model of resiniferatoxin-induced small-fiber sensory neuropathy (13), raising the possibility that 4MC might also enhance regeneration after crush injury.

In this report, we assessed whether the extents of muscular and cutaneous reinnervation are similar in the hind paw of mice after sciatic nerve crush injury and whether 4MC can enhance nerve regeneration of motor versus sensory nerves after this injury.

From the Department of Anatomy and Cell Biology (Y-LH, W-ML, J-HL, M-FC, S-TH), College of Medicine, National Taiwan University, Taipei; Department of Anatomy, School of Medicine (Y-LH), College of Medicine, Kaohsiung Medical University, Kaohsiung; and Department of Neurology (S-TH), National Taiwan University Hospital, Taipei, Taiwan.

Send correspondence and reprint requests to: Sung-Tsang Hsieh, MD, PhD, Department of Anatomy and Cell Biology, College of Medicine, National Taiwan University, 1 Jen-Ri Rd, Sec 1, Room No. 638, Taipei, 10051, Taiwan; E-mail: shsieh@ntu.edu.tw

This work was supported by the National Health Research Institute (NHRI-EX97-9736NI) and the National Science Council of Taiwan (NSC96-2320-B-002-002) to Sung-Tsang Hsieh and the Kaohsiung Medical University Research Foundation (KMU-Q098015) to Yu-Lin Hsieh.

MATERIALS AND METHODS

Animal Surgery

A crush injury to the sciatic nerve was performed on 8-week-old adult male ICR mice weighing 35 to 40 g. Mice were anesthetized with 4% chloral hydrate (400 mg/kg). A skin incision was made at the midthigh level of the hindlimb on 1 side. The gluteus and biceps femoris muscles were carefully separated to expose the sciatic nerve; the nerve was crushed with no. 5 forceps (Regine Switzerland, Morbio Inferiore, Switzerland) for 30 seconds; the contralateral sciatic nerve was left intact. Mice were housed in plastic cages on a 12-hour light/12-hour dark cycle and were able to access water and food ad libitum. All procedures were conducted in accordance with ethical guidelines set up by the National Research Council's guide for the care of laboratory animals (14) and the International Association for the Study of Pain on the use of animals in experimental research (15, 16). The protocol was approved by the Animal Committee of National Taiwan University College of Medicine, Taipei, Taiwan.

Experimental Design and the Administration of 4MC

In the first part of the study, we assessed the degree of denervation on postoperative day 7 (POD7) and reinnervation at postoperative month 1 (POM1) in the skin and muscle. In the second part, we investigated whether 4MC treatment promoted reinnervation of the skin or muscles at POM3. To examine the effects of 4MC, mice with a crush injury were divided into 2 groups. In the treatment group, 4MC (Wako, Osaka, Japan) was dissolved in PBS and administered by intraperitoneal injection (10 μg/kg) every morning beginning from the day after the injury to POM3 as described before (13). The control group received PBS following the same schedule.

Immunohistochemistry of Footpads

For immunostaining of the footpad skin, mice were perfused with 4% paraformaldehyde. The procedures followed published protocols (17). Tissues were removed and postfixed in the same fixative for 6 hours and then changed to PB for storage. After thorough rinsing in PBS, tissues were cryoprotected with 30% sucrose in PBS overnight. Sections (30 μm) were cut perpendicular to the epidermis on a HM440E sliding microtome (Microm, Walldorf, Germany), sequentially labeled, and stored at −20°C in antifreeze. To ensure adequate sampling, every third section of each footpad and 5 sections were chosen for immunohistochemistry. Sections were treated with 0.5% Triton X-100 in 0.5 mol/L Tris buffer (Tris, pH 7.6) for 30 minutes and processed for immunostaining. Briefly, sections were quenched with 1% H_2O_2 in methanol and blocked with 5% normal goat serum in 0.5% nonfat dry milk/Tris. Sections were incubated with rabbit antiserum to a pan-axonal marker, protein gene product 9.5 ([PGP9.5] 1:1000, UltraClone, Isle of Wight, UK). After rinsing in Tris, sections were incubated with biotinylated goat anti-rabbit immunoglobulin G (Vector, Burlingame, CA) for 1 hour and the avidin-biotin complex (Vector) for 1 hour. The reaction product was demonstrated by 3,3′-diaminobenzidine (Sigma, St Louis, MO), and sections were mounted on gelatin-coated slides.

Quantitation of Skin Innervation

PGP9.5(+) epidermal nerves were counted under 400× magnification (Axiophot microscope, Carl Zeiss, Oberkochen, Germany) following established criteria in a coded fashion (17). Epidermal nerves with branching points within the epidermis were counted as a single epidermal nerve. Each single epidermal nerve of epidermal nerves with branching points in the dermis was counted. The length along the lower margin of the stratum corneum was defined as the epidermal length and was measured with NIH image version 1.6.3 for Macintosh (NIH, Bethesda, MD). Epidermal nerve density (END) was expressed as the count of epidermal nerves divided by the epidermal length (fibers per centimeter). The *skin innervation index* was defined as the END of the operated side normalized to the contralateral side.

Quantitative Assessment of Neuromuscular Junctions

The innervation of the neuromuscular junctions (NMJs) in plantar muscles was evaluated with a combination of cholinesterase histochemistry and PGP9.5 immunostaining following established protocols (4). Briefly, the plantar muscles were carefully dissected and cryoprotected with 30% sucrose overnight. Serial sections (30 μm) were cut on a CM3050S cryostat (Leica, Wetzlar, Germany) and mounted on gelatin-coated slides. Every fifth section was stained with cholinesterase followed by PGP9.5. Briefly, plantar muscle sections were rinsed in Tris for 15 minutes and incubated in a 5-bromoindoxyl acetate solution for 15 minutes to demonstrate the cholinesterase in NMJs followed by PGP9.5 immunohistochemistry. Coded sections from the operated and contralateral side were examined, and 20 fields were randomly selected from each side of plantar muscle sections under an Axiophot microscope at 200× magnification. The NMJ innervation ratios were calculated by the number of innervated NMJs divided by the number of total NMJs on all stained sections. The *NMJ innervation index* was defined as the NMJ innervation ratio of the operated side normalized to the contralateral side.

Nerve Morphometry

Morphometric analyses of myelinated and unmyelinated nerve fibers were performed on sural nerves (13). Briefly, sural nerves were dissected after intracardiac perfusion with 5% glutaraldehyde and further fixed for another 2 days in the same fixative. After rinsing in PB, tissues were postfixed in 2% osmium tetroxide for 2 hours, dehydrated through a graded ethanol series, and embedded in Epon 812 resin (Polyscience, Philadelphia, PA). Semithin and thin sections were cut on an ultramicrotome (Reichert Ultracut E; Leica). Semithin sections were stained with toluidine blue. For myelinated morphometry, photographs were taken at a magnification of 400× under an Axiophot microscope; and fiber density, histograms of fiber diameters, and *g* ratios of myelinated fibers were determined. The *myelinated nerve fiber density* was defined as the total number of myelinated

TABLE. Primers and Conditions Used in Reverse Transcription–Polymerase Chain Reaction

Molecule	Forward Sequence	Backward Sequence	Size, bp	Thermal Cycles
NGF	ATACTGCACCACGACTCACAC	CTCTTCTTGTAGCCTTCCTGCT	103	27
GDNF	ACCTCTTCCTCTATCCTTGCC	AAACAATGAGGGAGGGCCTCT	212	28
BDNF	GAAAGTCCCGGTATCCAAAG	CCAGCCAATTCTCTTTTT	181	29
NT3	ATGCAGAACATAAGAGTCAC	AGCCTACGAGTTTGTTGTTTT	294	28
G3PDH	TGTGGCGTGATGGTCATGGG	GCACGTCAGATCCACGACAG	135	23

G3PDH, glyceraldehyde-3-phosphate dehydrogenase; GDNF, glial cell line-derived neurotrophic factor; BDNF, brain-derived neurotrophic factor; NGF, nerve growth factor; NT3, neurotrophin 3.

fibers divided by the area of the cross section of the sural nerves. The *g ratio* of each myelinated fiber was defined as the axon diameter divided by the fiber diameter. Cross-sectional areas of nerve fascicle, axon, and fiber diameter were measured by Image Pro-Plus software (Media Cybernetics, Bethesda, MD). Thin sections were stained with uranyl acetate and lead citrate, observed under an electron microscope (Hitachi H-7100, Tokyo, Japan) and photographed. For ultrastructural morphometry, electron microscopic photographs were taken in a systematic fashion at 8,000× magnification. A montage was created from all photographs. Areas of each montage covered 60% to 75% of the entire cross section of a sural nerve. Numbers of unmyelinated fibers enclosed within the basal lamina of a single Schwann cell (i.e. a Remak bundle) were counted for comparison. The *density of Remak bundles* and the *density of unmyelinated fibers* were defined as the number of Remak bundles (bundles per square millimeter) and unmyelinated fibers divided by the area of the endoneurium (fibers per square millimeter), respectively.

Neurophysiology of Motor Nerves

Sciatic nerves were exposed for nerve conduction studies as described (13). Briefly, a monopolar stimulating needle electrode was inserted at the sciatic notch. Surface recording electrodes were placed on the plantar surface to

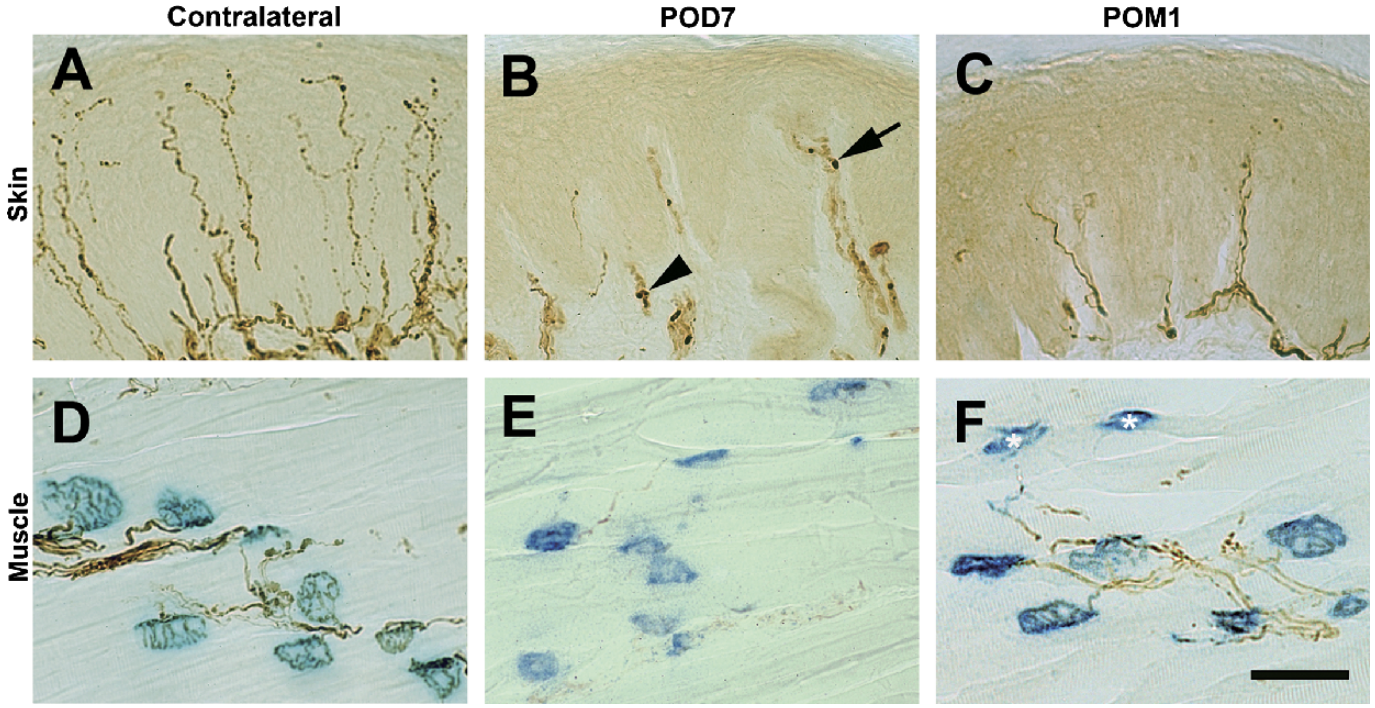

FIGURE 1. Skin and muscle innervation after sciatic nerve crush injury. **(A–C)** Epidermal nerves are demonstrated by immunohistochemistry using the pan-axonal marker protein gene product 9.5 (PGP9.5) on footpad skin. **(D–F)** Innervation of neuromuscular junctions (NMJs) was shown by acetylcholine histochemistry and PGP9.5(+) on plantar muscles. **(A)** On the contralateral side, PGP9.5(+) epidermal nerves arise from the subepidermal nerve plexus and have a typical varicose appearance. **(B)** On postoperative day 7 (POD7), most epidermal nerves have disappeared. The remaining epidermal nerves (arrow) and subepidermal plexus (arrowhead) have a fragmented appearance. **(C)** PGP9.5(+) epidermal nerves have reappeared by postoperative month 1 (POM1). **(D)** On the contralateral side, overlap of NMJs (blue) and PGP9.5(+) nerves (brown) indicates that the muscle is innervated. **(E)** On POD7, nearly all NMJs have become denervated. **(F)** Most NMJs are reinnervated by POM1, with only rare NMJs remaining denervated (white asterisks). Scale bars = 50 μm.

record compound muscular action potentials (CMAPs) with the Nicolet VikingQuest System (Nicolet Biomedical, Madison, WI). A monopolar electrode was inserted into the mouse tail as the ground electrode. Amplitudes of CMAPs were calculated for analyses.

Reverse Transcription–Polymerase Chain Reaction

Reverse transcription–polymerase chain reaction (RT-PCR) was performed in the epidermis of the hind paw skin following established protocols (18). Briefly, tissues were homogenized with an RNeasy Mini Kit (QIAGEN). The RNA pellets were resuspended with water to make cDNA with Thermoscript RT-PCR system (Invitrogen, Carlsbad, CA). The PCR reactions were carried out using Taq DNA polymerase Master Mix RED (Ampliqon, Copenhagen, Denmark) and primers for NGF, GDNF, brain-derived neurotrophic factor (BDNF), and neurotrophin 3 (Table) in a GeneAmp PCR system (PE Applied Biosystems, Foster City, CA). Different thermal cycles of PCR were used to ensure that the quantitation was in the linear range (20–30 cycles). For quantitation, we performed PCR with the parameters initial denaturation at 95°C for 1 minute and various thermal cycles (95°C for 15 seconds and 60°C for 60 seconds) for each neurotrophin followed by extension at 72°C for 6 minutes. The PCR products were resolved on 1.2% agarose gels and stained with ethidium bromide. The intensities of bands were quantified with GelPro (Media Cybernetics, Silver Spring, MD) and normalized to those of glyceraldehyde-3-phosphate dehydrogenase bands following our established quantitation protocol (19). To avoid run-to-run variations, all tissues were processed at the same time. Appropriate positive and negative controls were included at each step, that is, RNA extraction, cDNA synthesis, and PCR.

Statistical Analysis

Each group of animals received the same care, and 5 animals were used for each assessment at each time point. To eliminate concerns about individual variations among animals, data of the operated side were normalized to the contralateral side as an index, for example, the skin innervation index and muscle innervation index. All data are expressed as the mean ± SD. Means between 2 groups or 2 time points were analyzed with *t*-test; $p < 0.05$ was considered to be significant.

RESULTS

Denervation of Skin and Muscle After Crush Injury

To compare cutaneous and muscular innervation after crush injury, we examined the footpad skin and plantar muscle on POD7 and at POM1. Epidermal nerves on the contralateral side arose from the subepidermal plexus and had a varicose appearance (Fig. 1A). On POD7, almost all epidermal nerves had disappeared, and there were swollen or fragmented nerve fibers in the subepidermal plexus, compatible with denervation (Fig. 1B). At POM1, there were a few nerves indicating reinnervation (Fig. 1C).

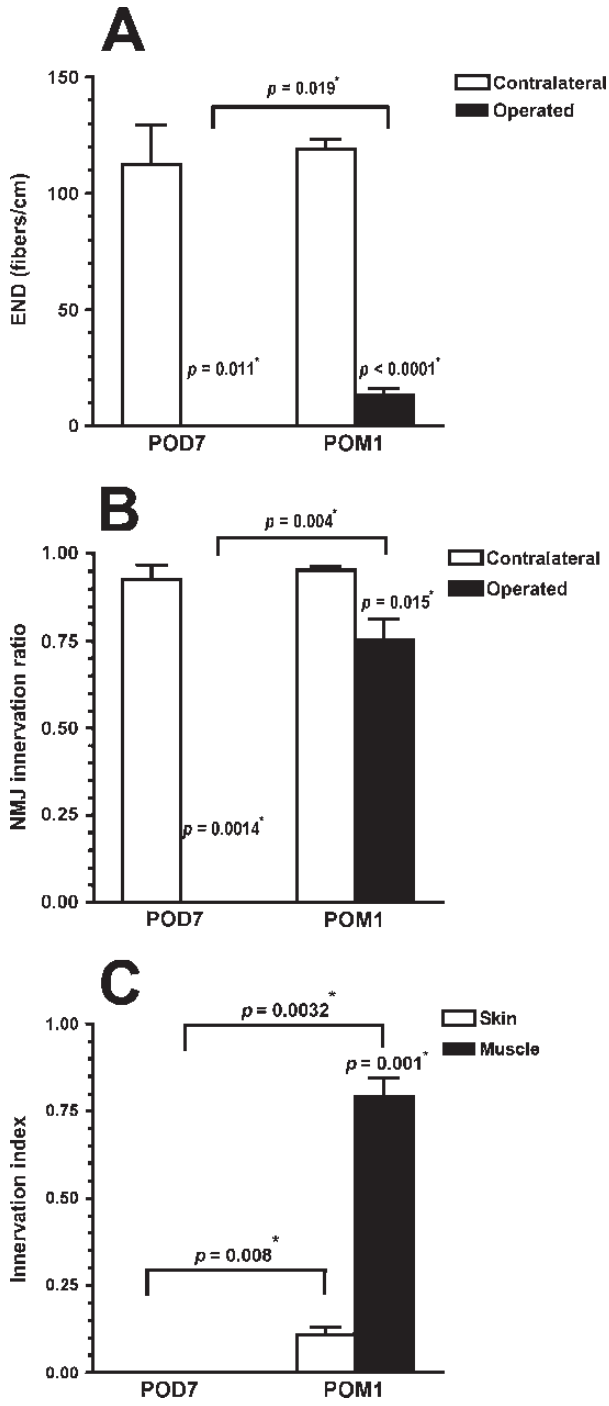

FIGURE 2. Quantification of skin and muscle innervation after sciatic nerve crush injury. **(A, B)** Histopathologic changes were quantified as epidermal nerve density (END) for skin innervation **(A)** and the neuromuscular junction (NMJ) innervation ratio for muscle innervation **(B)** on postoperative day 7 (POD7) and at postoperative month 1 (POM1). **(C)** The data were further normalized to the contralateral side as the skin innervation index (open bar) and muscle innervation index (black bar). *Indicates significant differences with indicated p values.

In plantar muscles on the contralateral side, PGP9.5 immunoreactivity appeared in nerve bundles; their branches were superimposed on NMJs, indicating that NMJs were innervated (Fig. 1D). On POD7, PGP9.5(+) nerve bundles and NMJs were absent (Fig. 1E), but they reappeared at POM1 (Fig. 1F).

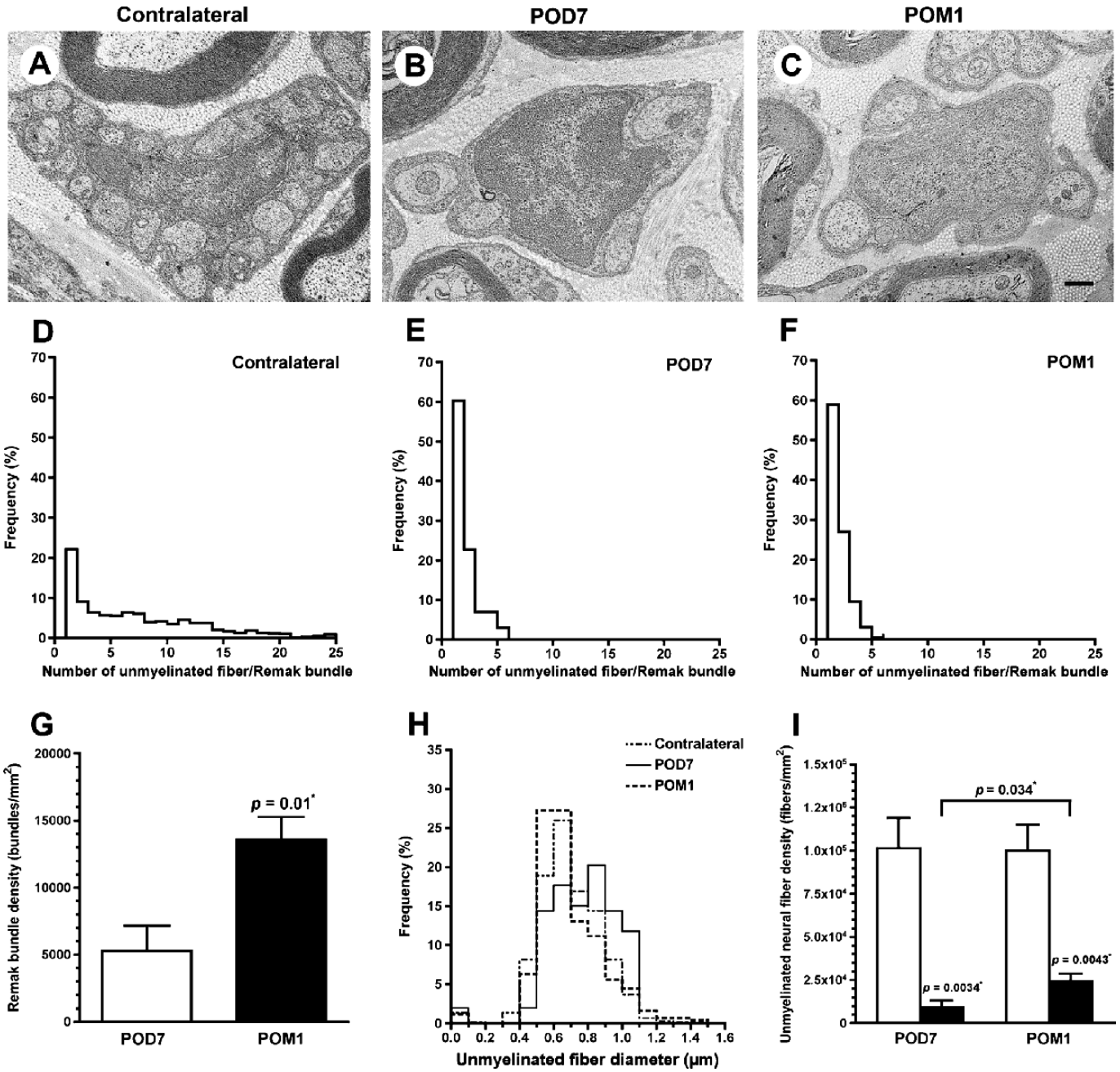

FIGURE 3. Ultrastructural morphometric analyses of unmyelinated nerve fibers after sciatic nerve crush injury. **(A–C)** Ultrathin sections of sural nerves were examined by electron microscopy. **(D–I)** The findings were quantified according to the number of unmyelinated fibers/Remak bundle **(D–F)**, the Remak bundle density **(G)**, the histogram of unmyelinated fibers **(H)**, and the unmyelinated fiber density **(I)** on postoperative day 7 (POD7) and at postoperative month 1 (POM1) after injury. On the contralateral side, several unmyelinated nerve fibers are enclosed by a single Schwann cell, forming a Remak bundle **(A)**. Most enclosed unmyelinated fibers have disappeared by POD7 **(B)**, and only rare enclosed unmyelinated fibers can be recognized at POM1 **(C)**. The histogram pattern of unmyelinated fiber/Remak bundle shows a left-shifted tendency on POD7 **(E)** and at POM1 **(F)** compared with that on the contralateral side **(D)**. The Remak bundle density at POM1 is higher than that on POD7 **(G)**. The spectrum of unmyelinated nerve fiber diameters is shifted to the right on POD7 **(H)**. The unmyelinated nerve fiber density **(A–C)** was quantitated **(I)**. *Significant differences with p values indicated. Scale bars = **(A–C)** 500 nm.

On POD7, the epidermis was completely denervated compared with the contralateral side with END of 0.00 ± 0.00 versus 112.30 ± 29.87 fibers/cm, respectively ($p = 0.011$). There was a mild increase in the END at POM1 compared with that on POD7 (13.19 ± 7.05 fibers per centimeter, $p = 0.019$), but this was still much lower than that on the contralateral side ($p < 0.0001$; Figs. 1A, C; 2A).

In plantar muscles, the NMJ innervation ratio was 0.93 ± 0.08 on the contralateral side; the value dropped to 0.00 ± 0.00 on POD7 after crush ($p = 0.0014$). At POM1, the NMJ innervation ratio had significantly increased compared with that on POD7 (0.76 ± 0.12 vs 0.00 ± 0.00; $p = 0.004$), but this was still lower than that on the contralateral side ($p = 0.015$) (Fig. 2B).

To standardize the comparison of cutaneous and muscular innervation, we used the skin innervation index and muscle innervation index (Fig. 2C). There was significant reinnervation from POD7 to POM1 ($p = 0.008$ for the

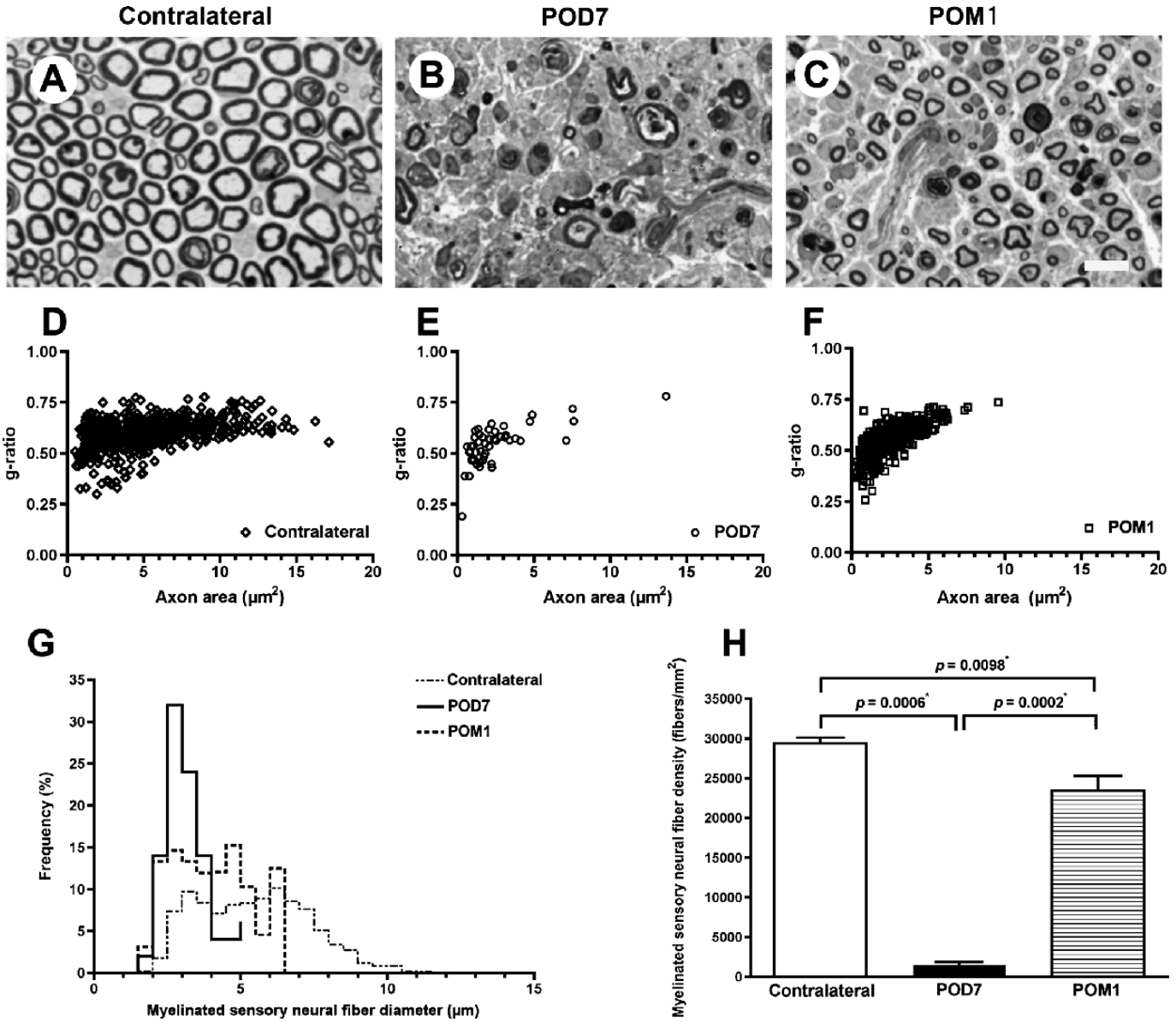

FIGURE 4. Pathology and morphometry of myelinated fibers in sural nerves after sciatic nerve crush injury. **(A–C)** Semithin sural nerve sections from postoperative day 7 (POD7) and at postoperative month 1 (POM1) were stained with toluidine blue. **(D–H)** Morphometric analyses of myelinated fibers included *g* ratio analyses **(D–F)**, histogram of fiber diameters **(G)**, and density of myelinated fibers **(H)**. **(A)** Sural nerve on the contralateral side contains large and small myelinated fibers. **(B)** Almost all myelinated fibers have degenerated on POD7. **(C)** Regenerating myelinated fibers appear by POM1. The *g* ratios of myelinated fibers on POD7 **(E)** and POM1 **(F)** are similar to those of the contralateral side **(D)**. **(G)** The ranges of myelinated fiber diameters are shifted to the left on POD7 and POM1. **(H)** Statistical comparison of myelinated fiber densities. *Significant differences with p values indicated. Scale bars = **(A–C)** 10 μm.

skin and p = 0.0032 for the muscle). Muscle reinnervation was relatively better than skin reinnervation (p = 0.001) (Fig. 2C).

Ultrastructural Morphometry of Unmyelinated Fibers After Crush Injury

By electron microscopy, several unmyelinated fibers were enclosed by a single Schwann cell, forming a Remak bundle (Fig. 3A) on the contralateral side. Most unmyelinated fibers had disappeared on POD7 (Fig. 3B), and some unmyelinated fibers had reappeared at POM1 (Fig. 3C). There were 7.40 ± 1.17 unmyelinated fibers/Remak bundle on the contralateral side (Fig. 3D), with a marked reduction on POD7 (1.61 ± 0.36 unmyelinated fibers/Remak bundle) (Fig. 3E). At POM1, this value remained stable (1.61 ± 0.11 unmyelinated fibers/Remak bundle), but the sural nerve had a higher Remak bundle density compared with that on POD7 (Figs. 3F, G), reflecting the proliferation of Schwann cells after nerve injury. Compared with the contralateral side, the mean diameter of unmyelinated fiber was shifted to the right on POD7 (0.64 ± 0.05 vs 0.78 ± 0.02 μm, p = 0.02) but not on POM1 (0.65 ± 0.04 μm, p = 0.70; Fig. 3H). The unmyelinated fiber density was markedly reduced on POD7 (101,560 ± 34,805 vs 8,960 ± 7,199 fibers/mm^2, p = 0.0034); this value was increased at POM1 compared with that on POD7 (24,150 ± 7,841 vs 8,960 ± 7,199 fibers/mm^2, p = 0.034) but was still lower than that on the contralateral side (p = 0.0043) (Fig. 3I).

Histopathology of Myelinated Sural Nerve Fibers

Sural nerves on the contralateral side were composed of large and small myelinated fibers (Fig. 4A). Myelinated fibers were almost absent on POD7, with only axonal and myelin debris visible (Fig. 4B); those fibers reappeared on POM1 (Fig 4C). Quantitatively, the *g* ratios were similar on POD7 (0.54 ± 0.02) and POM1 (0.56 ± 0.04) compared with the contralateral side (0.58 ± 0.01, p = 0.06 for POD7 and p = 0.70 for POM1; Figs. 4D–F). Myelinated fibers on POD7 and POM1 were smaller as the ranges of myelinated fiber diameters were shifted to the left (Fig. 4G). The myelinated fiber density was lowest on POD7 (29,377 ± 1,473 vs 1,456 ± 767 fibers/mm^2; p = 0.0006). At POM1, there was an increase in myelinated fiber density compared with POD7 (p = 0.0002), but the value was lower than that on the contralateral side (23,433 ± 3,157 fibers/mm^2; p = 0.0098) (Fig. 4H).

Effect of 4MC on Cutaneous and Muscular Reinnervation

To evaluate the effect of 4MC on patterns of reinnervation, we assessed the skin and muscle innervation at POM3.

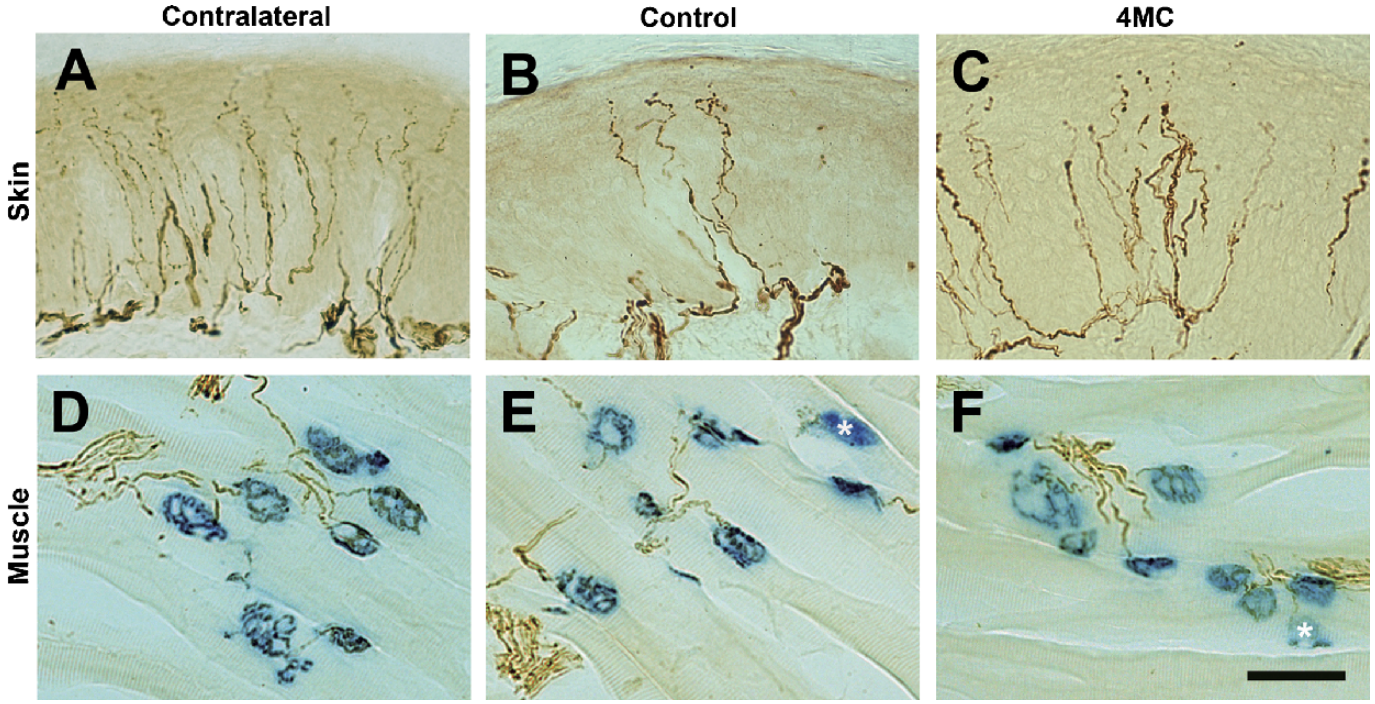

FIGURE 5. Effects of 4-methylcatechol (4MC) on reinnervation of skin and muscle at postoperative month 3 (POM3) after sciatic nerve crush injury. **(A–C)** At POM3, skin innervation was demonstrated with protein gene product 9.5 (PGP9.5) immunohistochemistry in the footpad skin. **(D–F)** Muscle reinnervation is shown by cholinesterase histochemistry for neuromuscular junctions ([NMJs] blue) and PGP9.5 immunohistochemistry (brown) for nerves. Panels are from the contralateral side **(A, D)**, the control treatment group **(B, E)**, and the 4MC group **(C, F)**. **(A–C)** There are more epidermal nerve fibers after 4MC treatment compared with the control treatment, but there are fewer PGP9.5(+) epidermal nerves in the 4MC group than on the contralateral side. Patterns of innervated NMJs in the control **(E)** and 4MC groups **(F)** are similar, with only a few denervated NMJs (white asterisks) compared with those on the contralateral side **(D)**. Scale bars = 50 μm.

In the 4MC group, there were more epidermal nerves than in the control group (Figs. 5A–C). This observation was corroborated by quantitation of the END; the END was higher in the 4MC group than in the control group (56.92 ± 12.66 vs 35.28 ± 12.95 fibers/cm, $p = 0.011$) but was lower than that on the contralateral side (126.70 ± 18.42 fibers/cm, $p < 0.0001$) (Figs. 5A–C; 6A). Similarly, the normalized skin innervation index in the 4MC group was higher than that of the control group (0.47 ± 0.05 vs 0.28 ± 0.06, $p = 0.0002$) (Fig. 6C).

In contrast, the patterns of NMJ innervation were the same in both the 4MC and control groups (Figs. 5D–F). NMJ innervation ratios were the same between the 2 groups (0.78 ± 0.08 vs 0.78 ± 0.08; $p = 0.48$) but were lower than that on the contralateral side (Fig. 6B).

At POM3, values of the normalized muscle innervation index were similar in both groups (0.88 ± 0.11 for the 4MC group and 0.87 ± 0.10 for the control group, $p = 0.44$) and were higher than the skin innervation indexes in both groups ($p < 0.0001$). Thus, 4MC specifically increased reinnervation of the skin with no influence on muscular reinnervation.

Promotion of Unmyelinated Fiber Regeneration by 4MC

In the 4MC group, there were more unmyelinated nerve fibers enclosed by each Schwann cell compared with the control group (Figs. 7A–C). Quantitatively, the 4MC group had higher numbers of unmyelinated fibers per Remak bundle (2.81 ± 0.27 vs 1.85 ± 0.21; $p = 0.001$) (Figs. 7D–F) and a higher unmyelinated fiber density compared with the control group (55,267 ± 6,047 vs 38,323 ± 3,841 fibers/mm^2, $p = 0.0042$); this was still lower than that on the contralateral side (100,019 ± 29,975 fibers/mm^2, $p = 0.006$; Fig. 7I). The Remak bundle density ($p = 0.13$) and mean unmyelinated fiber diameter ($p = 0.45$) were similar between the control and 4MC groups (Figs. 7G, H), however. These qualitative and quantitative data are direct evidence that 4MC promoted the regeneration of unmyelinated nerve fibers.

Effect of 4MC on Myelinated Sensory Nerve Fibers

Morphometry patterns of sural nerve myelinated fibers were the same in the 4MC and control groups (Figs. 8A–C), and the *g* ratios of the 4MC and control groups (0.58 ± 0.02 vs 0.58 ± 0.04, $p = 1.00$) were not significantly different compared with the contralateral side (0.59 ± 0.02, $p = 0.86$ for control and $p = 1.00$ for 4MC group; Figs. 8D–F). The mean fiber diameters of the 4MC and control groups were similar (4.39 ± 0.23 vs 4.38 ± 0.29 μm, $p = 0.48$) but were smaller than those of the contralateral side (5.05 ± 0.21 μm, $p = 0.004$ for both groups). These results were reflected in a mild left shift in the ranges of the control and the 4MC groups compared with that of the contralateral side (Fig. 8G). Both groups also had similar myelinated fiber densities (26,570 ± 6,711 vs 25,740 ± 1,711 fiber/mm^2, $p = 0.41$) that were comparable to that on the contralateral side (28,636 ± 2,819 fiber/mm^2, $p = 0.23$ for control group and $p = 0.09$ for

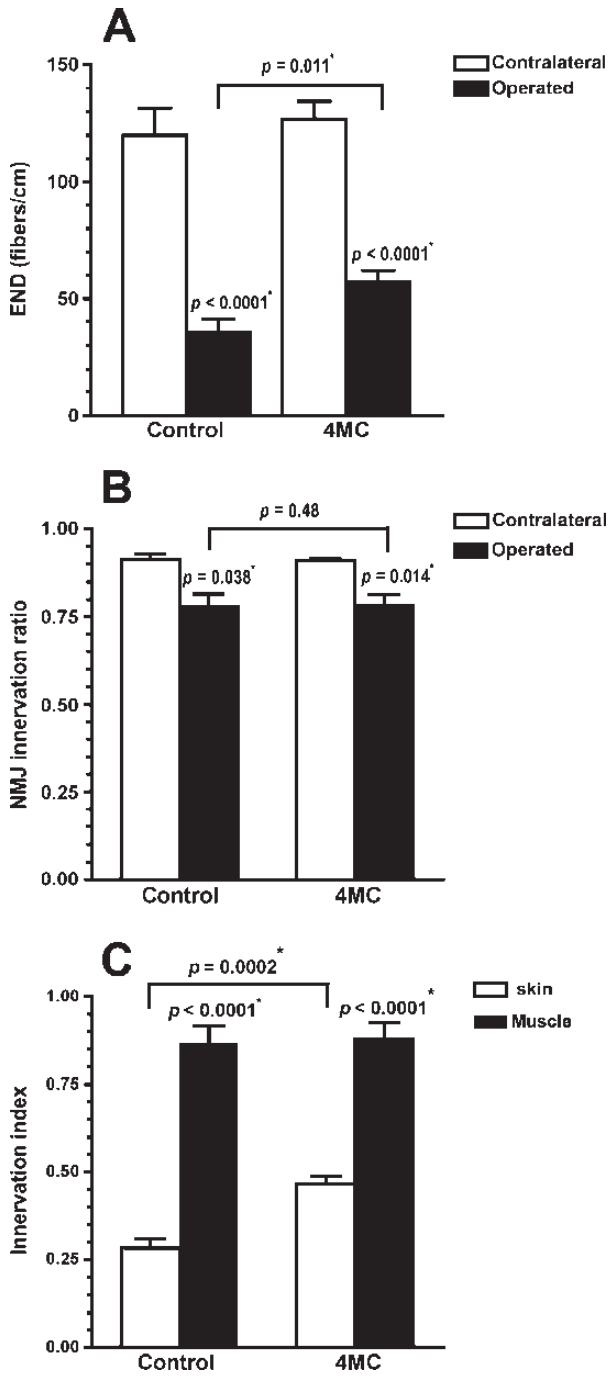

FIGURE 6. Quantification of skin and muscle innervation after 4-methylcatechol (4MC) treatment. **(A, B)** Differences in cutaneous and muscular reinnervation were quantified as the epidermal nerve density (END) for skin innervation **(A)** and the neuromuscular junction (NMJ) innervation ratio for muscle innervation **(B)** at postoperative month 3. **(C)** The data were further normalized to the contralateral side as the skin innervation index (open bar) and muscle innervation index (black bar). *Significant difference with indicated p values.

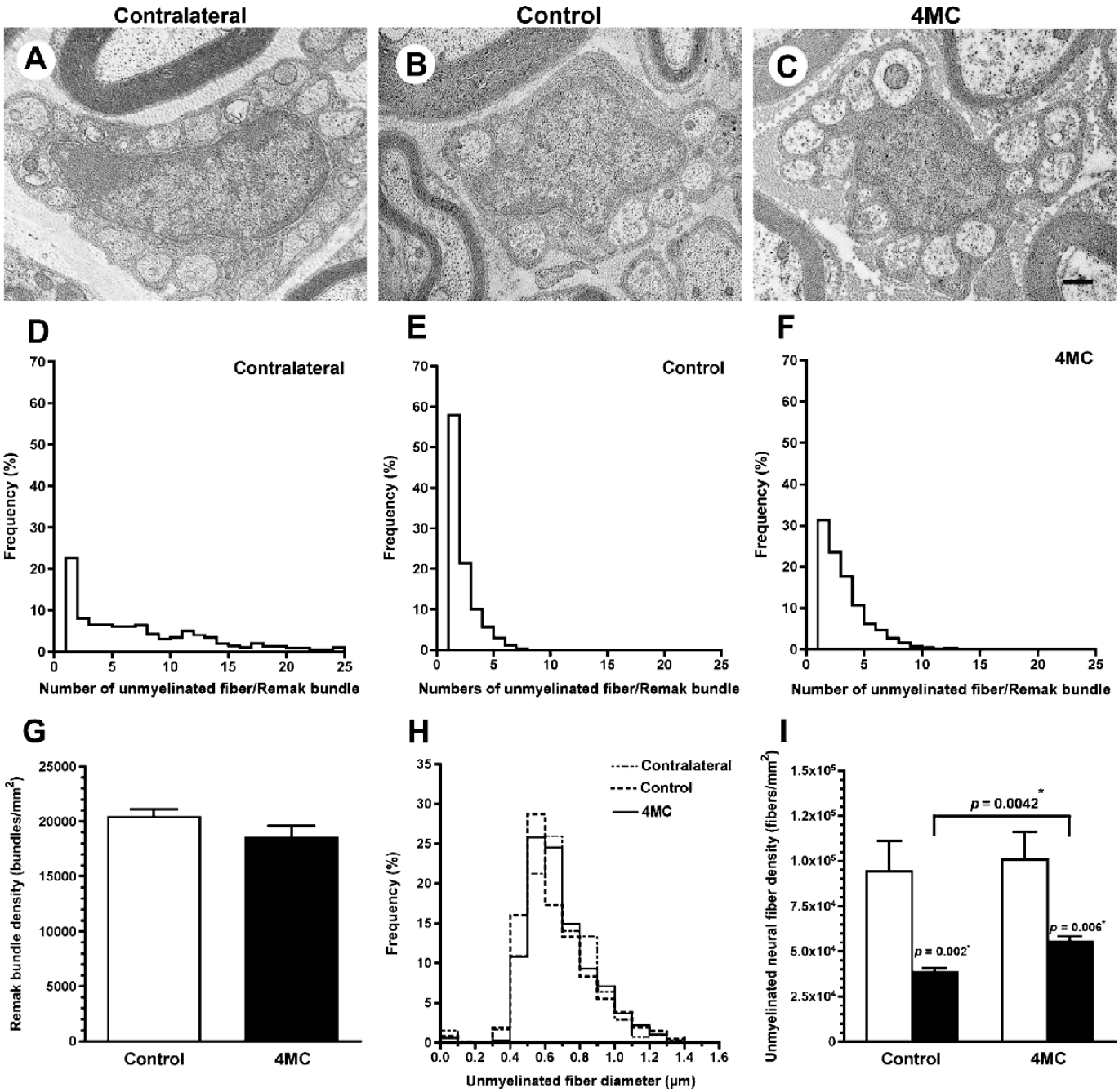

FIGURE 7. Ultrastructural morphometric analyses of unmyelinated nerve fibers after 4-methylcatechol (4MC) treatment. **(A–C)** Electron photomicrographs of sural nerves. **(D–F)** Numbers of unmyelinated fibers/Remak bundle on the contralateral side **(D)** and in the control **(E)** and 4MC **(F)** groups at postoperative month 3 (POM3). **(G)** Remak bundle density. **(H, I)** Histogram of unmyelinated fiber diameter **(H)** and unmyelinated fiber density **(I)**. On the contralateral side **(A)**, a Schwann cell encloses several unmyelinated fibers, forming a Remak bundle. There are fewer enclosed unmyelinated fibers in the control group **(B)** than in the 4MC group **(C)**. At POM3, the histogram of unmyelinated fibers/Remak bundle has a right-shifted pattern in the 4MC group compared with the control group (**[E]** vs **[F]**) but does not reach the pattern on the contralateral side **(D)**. Remak bundle densities are similar in the control and 4MC groups **(G)**. The histograms of unmyelinated fibers show similar patterns in both groups and comparable to the contralateral side **(H)**. Unmyelinated fiber density was quantitated according to the numbers of enclosed unmyelinated fibers as shown in **(A–C)**. Significant p values are indicated. Scale bars = **(A–C)** 500 nm.

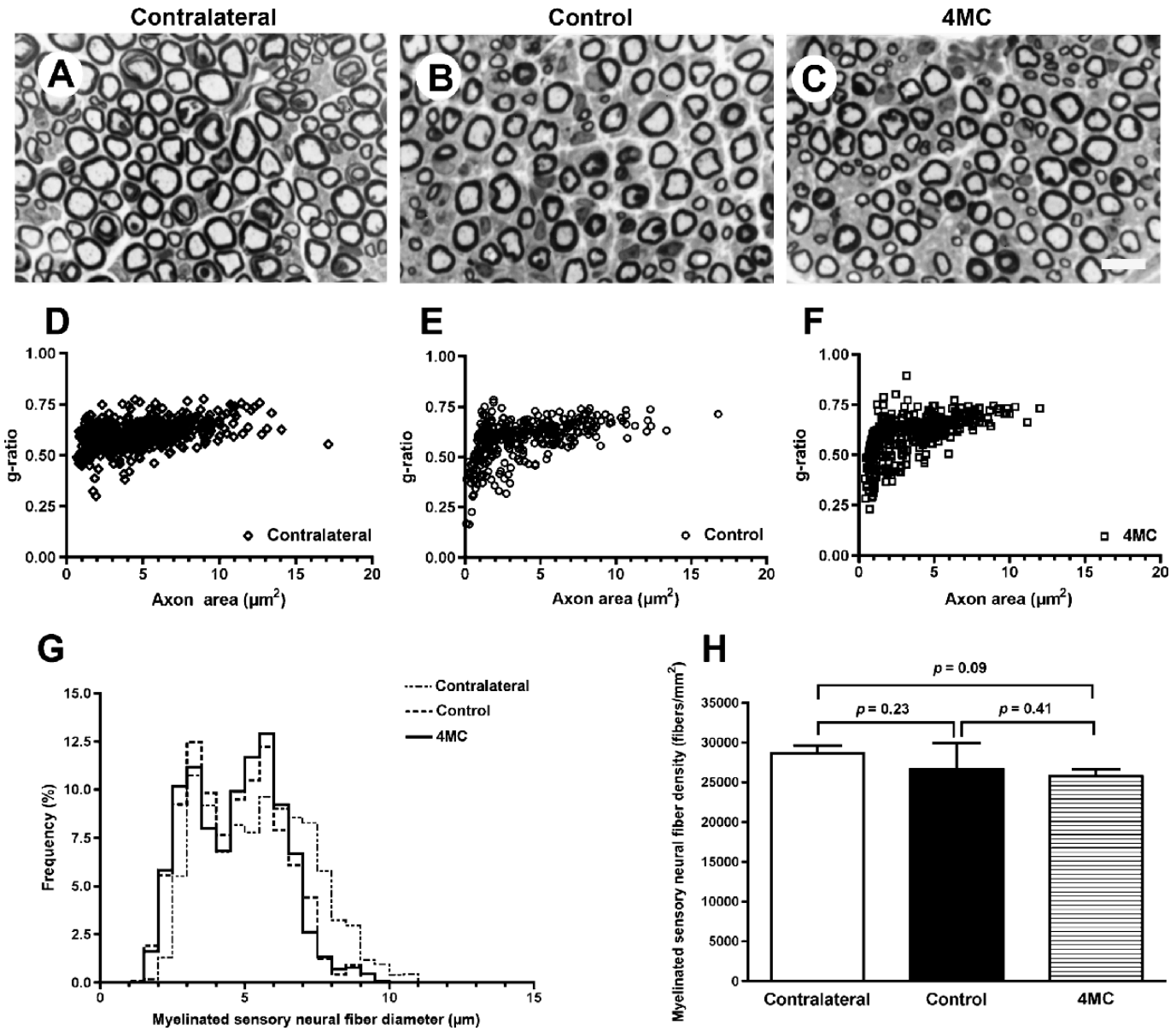

FIGURE 8. Morphometry of myelinated sural nerves after 4-methylcatechol (4MC) treatment. **(A–C)** Semithin sections of Epon-embedded sural nerves at postoperative month 3 stained with toluidine blue. **(D–H)** Morphometric analyses of myelinated fibers included *g* ratio analyses **(D–F)**, histograms of fiber diameter **(G)**, and fiber densities **(H)**. The patterns of myelinated fibers are similar in the contralateral **(A)**, control treated **(B)**, and 4MC **(C)** groups. The *g* ratio analysis shows similar patterns of myelinated fibers in the contralateral side **(D)**, control **(E)**, and 4MC **(F)** groups. Histograms of fiber diameter show a mild left shift in both the control and 4MC groups compared with the contralateral side **(G)**. Statistical comparison of fiber densities **(H)** with p values indicated. Scale bars = **(A–C)** 10 μm.

the 4MC group; Fig. 8H). This observation indicates that the regeneration of myelinated fibers was not influenced by 4MC.

Neurophysiology of Motor Nerves

Both the 4MC and control groups had the same patterns of CMAP waveforms (Figs. 9A–C), and CMAP amplitudes were similar in the 2 groups (7.35 ± 1.41 vs 7.60 ± 1.45 mV, p = 0.39), but they were smaller than that on the contralateral side (9.65 ± 1.76 mV, p = 0.012 for the control and p = 0.022 for the 4MC group; Fig. 9D). Together with the data on NMJ innervation, these findings indicate that 4MC had no effect on motor nerve regeneration.

Neurotrophin Expression

To investigate the changes in neurotrophin expression after the administration of 4MC, we performed RT-PCR on the skin (Fig. 10A). Quantitatively, the NGF transcripts were higher in the 4MC group than in the control group (2.33 ± 0.44 vs 1.42 ± 0.35, p = 0.0026; Fig. 10B), and the GDNF

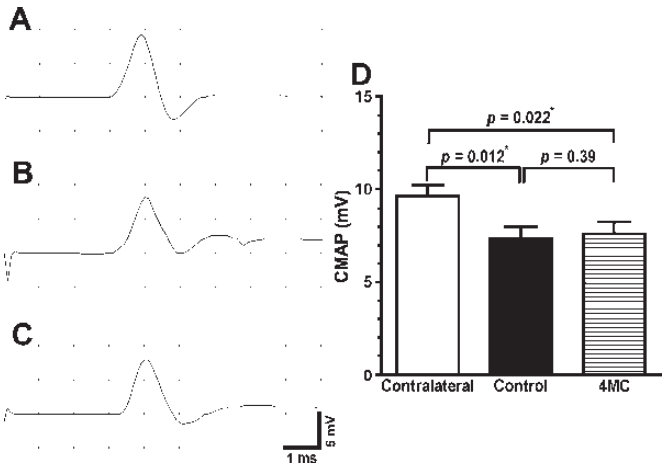

FIGURE 9. Nerve conduction studies of sciatic nerves after 4-methylcatechol (4MC) treatment at postoperative month 3. **(A–C)** Compound muscular action potentials (CMAPs) were recorded in plantar muscles on the contralateral side **(A)** and in the control **(B)** and 4MC groups **(C)**. **(D)** The CMAP amplitudes were measured and compared. The CMAP patterns are similar: the CMAP amplitudes are similar in the control and 4MC groups but are smaller than those on the contralateral side. *Significant p values are indicated.

transcripts showed a similar pattern (3.80 ± 0.97 vs 2.73 ± 0.37, p = 0.03; Fig. 10C). In contrast, the 4MC and control groups had similar amounts of the transcripts for BDNF (1.68 ± 1.25 vs 1.93 ± 1.02, p = 0.75; Fig. 10D) and neurotrophin 3 (1.77 ± 0.63 vs 1.60 ± 0.33, p = 0.58; Fig. 10E).

DISCUSSION

This study directly assessed targeted reinnervation after a crush injury and documents 2 important observations. First, muscular reinnervation is superior to cutaneous reinnervation after a sciatic nerve crush injury. Second, the application of 4MC promotes regeneration of unmyelinated nerves and consequent reinnervation of the skin.

The interpretation of nerve regeneration in previous studies mainly relied on morphometric measurements of the sciatic nerve (2, 7). With such an approach, it is impossible to compare the reinnervation of muscular and cutaneous targets. Only limited studies have compared the regeneration among nerve fibers of different types, particularly regeneration of unmyelinated nerves; the findings are inconsistent (20, 21). We demonstrated better muscular reinnervation compared with cutaneous reinnervation at POM3 after a crush injury. Because distance is a major determinant of nerve regeneration (22, 23), we compared innervation of the plantar muscles and of the hind paw skin because these targets are at similar distances from the site of nerve injury. The potential mechanisms underlying the difference in muscular and cutaneous reinnervation remain elusive, however. Several lines of evidence suggest a lesser ability for sensory nerves (i.e. large-diameter sensory nerves) compared with motor nerves to regenerate after nerve insults. Motor nerves achieve better functional recovery than sensory nerves as graft materials after a spinal cord injury (24), and the use of sensory nerves as a graft source of grafts showed a less regenerative potential compared with the use of motor nerves (25). One of the potential mechanisms may be related to differences in the size of the Schwann cell basal lamina tube (26). Alternatively, frequent contraction of muscles may induce a

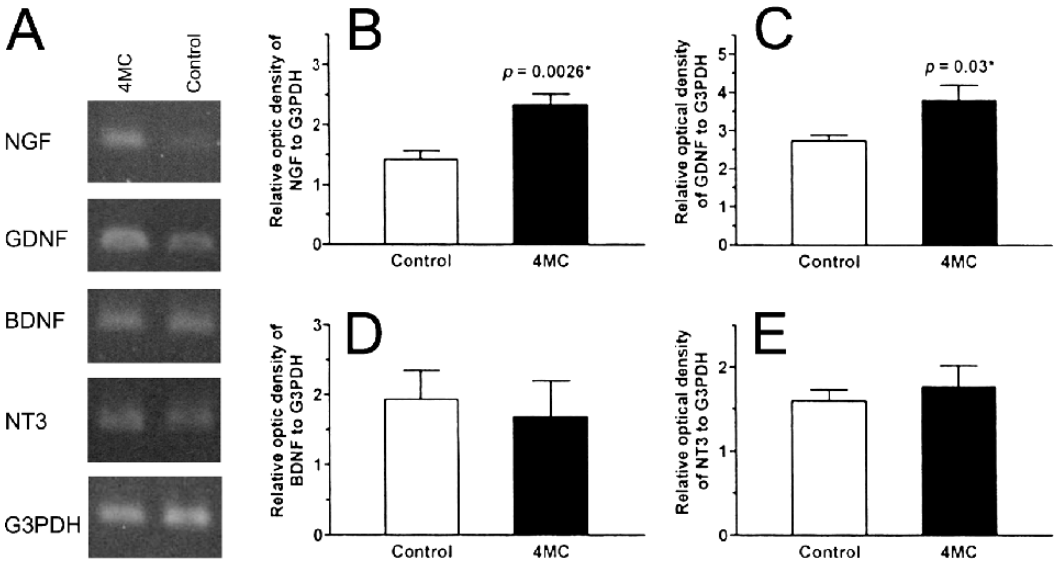

FIGURE 10. Effects of 4-methylcatechol (4MC) on neurotrophin expression. **(A)** Reverse transcription–polymerase chain reaction of the hind paw skin in the 4MC group and the control group was performed for nerve growth factor (NGF), glial cell line-derived neurotrophic factor (GDNF), brain-derived neurotrophic factor (BDNF), neurotrophin 3 (NT3), and glyceraldehyde-3-phosphate dehydrogenase (G3PDH). **(B–E)** The 4MC group had higher transcript levels of NGF **(B)** and GDNF **(C)**. Transcripts of BDNF **(D)** and NT3 **(E)** were similar in both groups. *Significant p values are indicated.

more powerful trophic effect on the regeneration of large myelinated fibers. In cross-grafting experiments, motor nerve fibers preferentially reinnervated the motor branches of injured nerves. The mechanisms for this remain unknown, and trophic factors likely play an important role (27). There are also significant changes in gene expression patterns of denervated muscles after transection. For example, neurotrophin BDNF and GDNF increase (28). In a model comparing the effect of nerve grafting, Michalski et al (29) documented that a mixed nerve (peroneal nerve) did better than a purely sensory nerve (saphenous nerve) in maintaining injury-induced upregulation of neurotrophins. However, these studies did not address the issue of whether regeneration of small-diameter sensory nerves, which reinnervate the skin, was poorer than that of large-diameter motor nerves, which reinnervate the muscles. The combination of assessments for muscular innervation and cutaneous innervation in this study provides an integrated approach to compare regeneration among nerves of different categories after injury.

We also demonstrate that cutaneous nerve regeneration was promoted by the intraperitoneal administration of 4MC. Because the muscular innervation index and morphometry of myelinated fibers in sural nerves were similar between the 4MC and control groups, this effect seems to be specific for small-diameter cutaneous nerves rather than large-diameter motor and sensory nerves. The regeneration of small-diameter cutaneous nerves after injury is a challenge, and to date, no satisfactory experimental or clinical approach has been reported to solve this problem. Recent advancements that take advantage of different mechanisms have enhanced peripheral nerve regeneration; these include vitamin D2 (30), etifoxine (31), fibroblast growth factor (32), vascular endothelial growth factor (33, 34), and keratin-enriched nerve conduits (35). So far, most studies assessed the morphometry of sciatic nerves or functional changes in gait to evaluate nerve regeneration. Despite some progress, there is no indication that small-diameter sensory nerves have successfully regenerated in those models. Cutaneous nerves are particularly vulnerable in human diabetic neuropathy in which sensory nerve degeneration develops earlier and more severely than motor deficits (6, 36).

The specific mechanisms of the beneficial effects of 4MC remain obscure. Initially, 4MC was identified as enhancing NGF synthesis (37); NGF is required for small-diameter dorsal root ganglion neurons, the peripheral processes of which terminate in the skin. In addition, 4MC can promote the phosphorylation of *trk*, a specific NGF receptor (38, 39). Based on similar principles, recent studies identified small molecules with similar effects on cultures of dorsal root ganglia neurons (40). In addition to NGF mRNA, we found that GDNF mRNA was also increased after 4MC treatment. Moreover, the proliferation of small unmyelinated fibers in the skin of 4MC-treated mice may reflect a terminal end organ effect on adrenergic nerves, passively induced by the 4MC therapy. This new finding suggests that the effect of 4MC may act through multiple trophic factors and pathways and offers a new direction for designing therapeutic strategies for cutaneous nerve regeneration.

ACKNOWLEDGMENTS

The authors thank the instrument support of the Department of Medical Research, Kaohsiung Medical University Hospital, Kaohsiung, Taiwan.

REFERENCES

1. Saxena S, Caroni P. Mechanisms of axon degeneration: From development to disease. Prog Neurobiol 2007;83:174–91
2. Carlstedt T. Root repair review: Basic science background and clinical outcome. Restor Neurol Neurosci 2008;26:225–41
3. Tannemaat MR, Eggers R, Hendriks WT, et al. Differential effects of lentiviral vector-mediated overexpression of nerve growth factor and glial cell line–derived neurotrophic factor on regenerating sensory and motor axons in the transected peripheral nerve. Eur J Neurosci 2008;28:1467–79
4. Chiang HY, Chien HF, Shen HH, et al. Reinnervation of muscular targets by nerve regeneration through guidance conduits. J Neuropathol Exp Neurol 2005;64:576–87
5. Tseng TJ, Chen CC, Hsieh YL, et al. Effects of decompression on neuropathic pain behaviors and skin re-innervation in chronic constriction injury. Exp Neurol 2007;204:574–82
6. Shun CT, Chang YC, Wu HP, et al. Skin denervation in type 2 diabetes: Correlations with diabetic duration and functional impairments. Brain 2004;127:1593–605
7. Navarro X, Vivo M, Valero-Cabre A. Neural plasticity after peripheral nerve injury and regeneration. Prog Neurobiol 2007;82:163–201
8. Jolivalt CG, Vu Y, Mizisin LM, Mizisin AP, Calcutt NA. Impaired prosaposin secretion during nerve regeneration in diabetic rats and protection of nerve regeneration by a prosaposin-derived peptide. J Neuropathol Exp Neurol 2008;67:702–10
9. Boucek P, Havrdova T, Voska L, et al. Epidermal innervation in type 1 diabetic patients: A 2.5-year prospective study after simultaneous pancreas/kidney transplantation. Diabetes Care 2008;31:1611–12
10. Kennedy JM, Zochodne DW. Impaired peripheral nerve regeneration in diabetes mellitus. J Peripher Nerv Syst 2005;10:144–57
11. Toth C, Brussee V, Cheng C, Zochodne DW. Diabetes mellitus and the sensory neuron. J Neuropathol Exp Neurol 2004;63:561–73
12. Zacchigna S, Lambrechts D, Carmeliet P. Neurovascular signalling defects in neurodegeneration. Nat Rev Neurosci 2008;9:169–81
13. Hsieh YL, Chiang H, Tseng TJ, Hsieh ST. Enhancement of cutaneous nerve regeneration by 4-methylcatechol in resiniferatoxin-induced neuropathy. J Neuropathol Exp Neurol 2008;67:93–104
14. National Research Council. *Guide for the Care and Use of Laboratory Animals*. Washington, DC: National Academy Press; 1996
15. IASP Committee. Ethical standards for investigations of experimental pain in animals. The Committee for Research and Ethical Issues of the International Association for the Study of Pain. Pain 1980;9:141–43
16. Zimmermann M. Ethical guidelines for investigations of experimental pain in conscious animals. Pain 1983;16:109–10
17. Hsieh ST, Chiang HY, Lin WM. Pathology of nerve terminal degeneration in the skin. J Neuropathol Exp Neurol 2000;59:297–307
18. Hsieh ST, Lin WM. Modulation of keratinocyte proliferation by skin innervation. J Invest Dermatol 1999;113:579–86
19. Lin YY, Tseng TJ, Hsieh YL, et al. Depletion of peptidergic innervation in the gastric mucosa of streptozotocin-induced diabetic rats. Exp Neurol 2008;213:388–96
20. Dvorakova MC, Pfeil U, Kuncova J, et al. Down-regulation of vasoactive intestinal peptide and altered expression of its receptors in rat diabetic cardiomyopathy. Cell Tissue Res 2006;323:383–93
21. Hofmann HA, De Vry J, Siegling A, Spreyer P, Denzer D. Pharmacological sensitivity and gene expression analysis of the tibial nerve injury model of neuropathic pain. Eur J Pharmacol 2003;470:17–25
22. Vivo M, Puigdemasa A, Casals L, Asensio E, Udina E, Navarro X. Immediate electrical stimulation enhances regeneration and re-innervation and modulates spinal plastic changes after sciatic nerve injury and repair. Exp Neurol 2008;211:180–93
23. Sosa I, Reyes O, Kuffler DP. Immunosuppressants: Neuroprotection and promoting neurological recovery following peripheral nerve and spinal cord lesions. Exp Neurol 2005;195:7–15
24. Chu TH, Du Y, Wu W. Motor nerve graft is better than sensory nerve

graft for survival and regeneration of motoneurons after spinal root avulsion in adult rats. Exp Neurol 2008;212:562–65.
25. Nichols CM, Brenner MJ, Fox IK, et al. Effects of motor versus sensory nerve grafts on peripheral nerve regeneration. Exp Neurol 2004;190:347–55
26. Moradzadeh A, Borschel GH, Luciano JP, et al. The impact of motor and sensory nerve architecture on nerve regeneration. Exp Neurol 2008; 212:370–76
27. Madison RD, Robinson GA, Chadaram SR. The specificity of motor neurone regeneration (preferential re-innervation). Acta Physiol (Oxf) 2007;189:201–6
28. Batt J, Bain J, Goncalves J, et al. Differential gene expression profiling of short and long term denervated muscle. FASEB J 2006;20:115–17
29. Michalski B, Bain JR, Fahnestock M. Long-term changes in neurotrophic factor expression in distal nerve stump following denervation and re-innervation with motor or sensory nerve. J Neurochem 2008;105: 1244–52
30. Chabas JF, Alluin O, Rao G, et al. Vitamin D2 potentiates axon regeneration. J Neurotrauma 2008;25:1247–56
31. Girard C, Liu S, Cadepond F, et al. Etifoxine improves peripheral nerve regeneration and functional recovery. Proc Natl Acad Sci U S A 2008; 105:20505–10
32. Grothe C, Haastert K, Jungnickel J. Physiological function and putative therapeutic impact of the FGF-2 system in peripheral nerve regeneration—lessons from in vivo studies in mice and rats. Brain Res Rev 2006;51: 293–99
33. Chattopadhyay M, Krisky D, Wolfe D, Glorioso JC, Mata M, Fink DJ. HSV-mediated gene transfer of vascular endothelial growth factor to dorsal root ganglia prevents diabetic neuropathy. Gene Ther 2005;12: 1377–84
34. Greenberg DA, Jin K. Neural gene therapy: Sensational finding. Gene Ther 2005;12:1161–62
35. Sierpinski P, Garrett J, Ma J, et al. The use of keratin biomaterials derived from human hair for the promotion of rapid regeneration of peripheral nerves. Biomaterials 2008;29:118–28
36. Said G, Baudoin D, Toyooka K. Sensory loss, pains, motor deficit and axonal regeneration in length-dependent diabetic polyneuropathy. J Neurol 2008;255:1693–702
37. Perez-Perez M, Garcia-Suarez O, Esteban I, et al. p75NTR in the spleen: Age-dependent changes, effect of NGF and 4-methylcatechol treatment, and structural changes in p75NTR-deficient mice. Anat Rec (Hoboken) 2003;270A:117–28
38. Sometani A, Nomoto H, Nitta A, Furukawa Y, Furukawa S. 4-Methylcatechol stimulates phosphorylation of Trk family neurotrophin receptors and MAP kinases in cultured rat cortical neurons. J Neurosci Res 2002;70: 335–39
39. Pezet S, McMahon SB. Neurotrophins: Mediators and modulators of pain. Annu Rev Neurosci 2006;29:507–38
40. Lin B, Pirrung MC, Deng L, Li Z, Liu Y, Webster NJG. Neuroprotection by small molecule activators of the nerve growth factor receptor. J Pharmacol Exp Ther 2007;322:59–69

